



Multi-characteristic overcurrent relay of feeder protection for minimum tripping times and self-protection

Abdallah Reda^{1,2} · Amal F. Abdelgawad³ · Mohamed I. Elsayed² · Fhaid B. Al-Dousar⁴

Received: 13 January 2022 / Accepted: 29 October 2022 / Published online: 30 December 2022
© The Author(s) 2022

Abstract

The main goal of this study is to propose new characteristics to an REF 615 model (overcurrent and earth fault relay) that is used for feeder protection in an actual radial system of an Egyptian Substation. When studying fault current, both light and heavy loads as well as fault locations are considered based on the radial nature of the network. The proposed algorithm relies on simultaneously activating the three settings of REF 615 OC relay, with the three settings being set on the respective normal inverse (NI), very inverse (VI) and definite time (DMT) curves. The relay's operating area is divided into two areas. The VI curve functions as a backup for NI in the first area, whereas the NI curve functions as a backup for VI in the second area. The novelty of this study is the proposed model's ability to handle relay failure through its self-protection, which increases the network's protection level and minimizes the relay operating time by about 41.07% for rapid response to a fault. The presence of self-backup protection can minimize the coordination time interval between the main protection and backup protection (CTI) by about 77.98%. The ETAP software is used to investigate the actual radial system and in the analysis of the protection coordination.

Keywords Protection coordination · Overcurrent relays · Nonstandard relay · ETAP software

Abbreviations

OC	Overcurrent
DG	Distributed generation
PCS	Pick-up current setting
FACTS	Flexible ac transmission system
DOCR	Directional overcurrent relay
FOCR	Factory overcurrent relay
SOCR	Substation overcurrent relay
DMT	Definite minimum time
IDMT	Inverse definite minimum time
CTI	Coordination time interval
FCL	Fault current limiter

✉ Abdallah Reda
eng.abdallahpower13@gmail.com

¹ El-Marg High Institute of Engineering and Modern Technology, Cairo, Egypt

² Department of Electrical Power and Machines Engineering, Faculty of Engineering, Al-Azhar University, Cairo, Egypt

³ Department of Electrical Power and Machines Engineering, Faculty of Engineering, Zagazig University, Sharkia, Egypt

⁴ General Authority for Vocational Training, Adailiyah, Kuwait

1 Introduction

1.1 Objective and motivation

A system under fault requires backup protection in addition to primary protection. This is because if the primary protection fails to operate and separate the fault, the backup protection can do so by acting in response to disturbance. In other words, each relay requires other relays to function as a backup. The first objective of this study is to develop a proposed model with backup protection against itself.

There are two types of relay curves: definite time and inverse time curves. The main advantage of inverse time curve is that higher fault currents meet shorter operating time. The second objective of this study is to design a proposed model that can improve the response of overcurrent (OC) relay by minimizing the tripping times during fault compared with the conventional model. Therefore, the inverse characteristics of the REF 615 OC relay are studied to achieve the main objectives of this study.

1.2 Literature review

Nonstandard curves can be used to improve the performance of OC relay. The authors of [2] propose the application of nonstandardized inverse time curves and distance relays to address the lack of sensitivity of relays during OC relay coordination. The OC relay model considers five adjustable settings to enhance the coordination when distance relays are considered. The proposed method minimizes the number of uncoordinated relays enabling improved implementation results. In [1], a directional OC relay coordination is performed considering multiple levels of short-circuit current and nonstandardized inverse time curves. A genetic algorithm is proposed and capable of obtaining adequate protection settings in a reasonable time. In [21], a protection coordination problem is formulated and solved to determine the optimal relay-tripping settings. The proposed approach is tested on an IEEE 24-bus transmission system. The results of this study revealed that protection schemes based on DOCRs controlled by the proposed tripping characteristic ensure fast fault isolations.

The presence of flexible AC transmission system (FACTS) controllers in transmission lines causes malfunction of distance relays. Series-shunt FACTS devices have a more significant influence on the performance of the relays compared with other FACTS controllers. In addition, a high-resistance fault is another factor that causes a relay to become underreach and incorrectly identify the fault. This study provides a method based on synchrophasors to eliminate the effects of a unified power-flow controller and fault resistance on the distance relay [9]. In addition, the insertion of DG into the network negatively impacts the protection coordination which might cause relays to lose their coordination. In [16], the noncommunication OC protection schemes do not allow backup relays to adequately coordinate with their primary relays. A method was proposed to determine the threshold value of the DG capacity, beyond which recloser-fuse coordination is lost. Mathematical equations for protective devices are used to set up the protection settings and to calculate the threshold value. The prospect of integrating optimal relay coordination methods with adaptive protection schemes (APSs) in the presence of DG was introduced in [19]. The effectiveness of the proposed strategy was assessed by simulating two DG-penetrated networks with various configurations. The protection coordination scheme discussed in [18] continuously monitors the state of the power network with or without DG. Depending on the network's operational topology of the network, time dial settings as well as plug settings of OC relays and setting of distance relays are selected from preoptimized relay group settings. New relay group settings are communicated to corresponding relays whenever there is any change in the network fault level either due to a change in line parameters or an incoming new distributed

energy resource. The distribution system in [20] suffers from the dynamic changes of the inputs and outputs of generators, lines and loads. The DOCRs were coordinated based on an ant colony algorithm-based adaptive protection strategy that was compared to a genetic algorithm. A method based on locally accessible measurements was presented in [23] to develop the functionality of the OC relay. It does not require any online information and communication facilities regarding changing the short circuit levels caused by distributed energy resource. This adaptive method uses a least square algorithm to determine the Thevenin circuit equivalent using local measurements.

In general, the current literature can be categorized into two classifications:

1. Adaptive protection scheme.
2. Non-adaptive protection scheme.

To remove the protective element's miscoordination using the non-adaptive OC protection scheme, the fault current limiter (FCL) was used to reduce the system's short circuit level to restore the original relay setting. This is an inexpensive scheme because it does not require other components unlike the adaptive protection scheme. Because of the robustness of that scheme, it might be inaccurate due to miscoordination's likelihoods and the backup relay's operating times are reasonably higher, which it sometimes does not operate at all. On the other hand, the failure chances in this scheme are low. Fault current limiter (FCL) is used in [8] to limit and reduce the distribution network's short circuit level in the presence of DG. The presence of both DG and FCL components causes transient currents during fault. Genetic algorithm introduces dynamic model for OC relays to achieve optimal relay setting.

In adaptive protection scheme, the relay settings were changed according to the network conditions. The adaptive protection scheme is based on activating the relay setting to adapt with the network's changes. The microprocessor-based relays and communication channel are required in this scheme. Although the adaptive protection scheme participates with excellent coordination, but it is very much dependent on communication link. Moreover, this adaptive protection scheme is an expensive due to the hardware's requirements. The authors in [11] propose the mitigation of the impact of DG impact on DOCR coordination by employing an APS using a differential evolution algorithm while improving the overall sensitivity of relays. The impacts of DG before and after the application of APS are presented based on an interconnected 6 bus and IEEE 14 bus system. Consequently, an overall sensitivity improvement and mitigation scheme has been proposed. In [12], the adaptive technique to OCRs is applied on the IEEE 14-bus test network and a 63/20 kV substation to demonstrate the efficiency of the

adaptive scheme verifies its effectiveness in reserving coordination for all topologies and lowering the relays' time dial setting. This technique can be implemented without involving the control center by making a computer network between the power network's substations using available communication links. In [17], an innovative adaptive directional OC protection system for electric power distribution systems based on distributed generation is proposed. The proposed system supervises network topology using the monitoring capabilities of numerical relays. The system detects any changes in the configuration and recalculates the directional OC protection settings using a microgenetic algorithm. The proposed system was evaluated for several operating scenarios and insertion levels of distributed generation and then compared with both conventional and adaptive protection systems using a traditional genetic algorithm. A full adaptive technique for setting all OC relays in HV substations is proposed in [22]. It is based on an appropriate equivalent circuit of the power grid in the substation, online estimation of the equivalent circuit parameters, and application of the equivalent circuit to estimate the required short-circuit currents. The technique is improved to address issues brought on by the penetration of distributed generation. Developing this adaptive setting technique is a step toward introducing self-adjustment OC relays. An adaptive OC protection that integrates the technical and economic advantages of fuses and relays in a microgrid with distributed generators is presented in [3]. This fuse relay adaptive OC protection scheme protects power lines and feeders by grouping identical inverse time OC settings of relays and logic gates of relay breakers.

Several optimization methods are proposed in [4–7, 10, 13–15] for solving the coordination problem which is described as a nonlinear programming. The study in [15] proposes a new time current voltage tripping characteristic for directional OC relays, which has the ability to reduce the relay's operating time in meshed distribution networks. In addition, the protection coordination problem has been implemented as a constrained nonlinear programming problem to achieve optimal relay settings. This study's results have been revealed that the updated DOCR's tripping characteristic achieves notable reduction in the operating time than the conventional characteristic. A metaheuristic algorithm is proposed in [6] to improve DOCR coordination. The proposed approach is tested on IEEE 30, 118, and 300 buses. The results improved the coordination performance and minimized the unwanted load shedding. An adaptive protection system by fuzzy logic that depends on the prefault current and current variation is proposed in [7]. The analysis is performed using the ATP EMTP software. This adaptive method based on logic and decision making provides more flexibility and high performance with automatic operation and high sensitivity of OC relays. A distribution system with DG is tested. The

nonlinear optimization model for solving the DOCRs coordination problem was presented in [4]. The main objective is to improve a modified version of the electromagnetic field optimization (EFO) algorithm to achieve DOCR's optimal coordination. The proposed algorithm has been applied to the 8, 9 and 15 buses test systems. A new approach based on the interval analysis was introduced in [5] to solve the DOCRs coordination problem considering uncertainty in the network topology. The DOCR coordination problem has been implemented as an interval linear programming (ILP) problem instead of the set of inequality constraints. The proposed method was applied to the IEEE 14 and 30 buses test systems. A multiobjective optimization algorithm is proposed in [13] to determine the optimum operation point considering the number of setting changes, setting groups and total protection time. A metaheuristic optimization method is proposed in [14]. There is a significant reduction in the relay's operation and pair-discrimination times. For a 30-bus power system, the total obtained relay operating time using the proposed method which satisfies highly reliable coordination is less than 1/10 of that obtained from conventional coordination methods. A hybrid method that combines fuzzy and genetic algorithms is used in [10] to update the relay settings. The proposed algorithm consists of a two-phase approach that deduces: optimal floating current settings through a fuzzy decision-making module and optimal floating time settings through an optimization algorithm. Extensive case studies have been conducted on the modified IEEE 14 and 30 bus power distribution networks by varying the type, location, and size of DGs.

1.3 Main contribution of this study

In the present study, the fault location, fault type and network configuration with light and heavy loads are considered in examining the fault current of an actual substation in Egypt during the coordination process. These fault conditions control the fault current value and can affect REF 615 relay's time setting. In addition, the actual REF 615 relay has been studied in the market and simulated using ETAP software. Three REF 615 settings were simultaneously used to design a nonstandard curve. The advantages of the proposed method over the conventional one are its simplicity in minimizing the operating time and the absence of any complex mixed methods to achieve optimal coordination. The first novel contribution of this study is that the nonstandard proposed model supports the relay using a tuning curve that functions as backup for itself. The presence of self-backup protection enables the relay to treat and deal with its failure while acting as the main protection, thus increasing the network's protection level. Moreover, the self-backup protection feature minimizes the coordination time interval by about 77.98%.

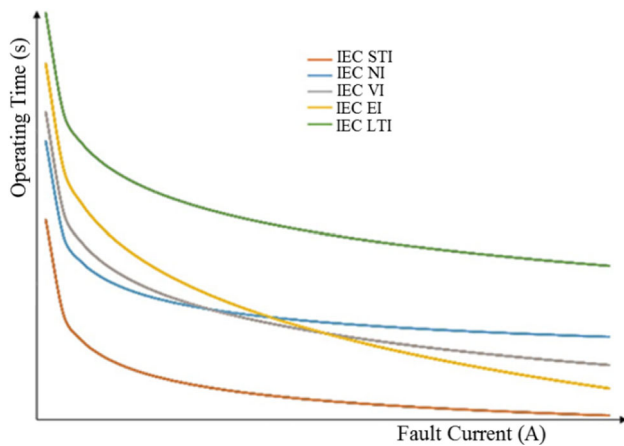


Fig. 1 IEC characteristics of OC relay

The second novel contribution of this study is that the proposed model minimizes the relay's operating time by about 41.07%.

1.4 Paper organization

The rest of this paper is structured as follows: Sect. 2 provides background information on the standard characteristics of the OC relay. Section 3 theoretically and practically illustrates the proposed method. Section 4 presents the analysis of the configuration of the studied network using the conventional relay model and the proposed technique. Section 5 provides the results of the proposed methodology. Section 6 discusses the results and presents the main achievements. Section 7 provides the conclusions of this study.

2 Standard characteristics of OC relay

This section gives brief description of the IEC and IEEE/ANSI standard characteristics of OC relay. The relay's standard features are described by an international approach of IEC [24] and IEEE [25] that defines the relay's characteristics using a mathematical expression [26] as illustrated in the following two subsections.

2.1 IEC standard characteristics

According to the international standard IEC 60,255, the relay curve is determined using Eq. (1). It is defined according to the relationship between the fault current and the trip time (Fig. 1). Table 1 provides the constants of Eq. (1) related to the REF 615 relay model (α and β).

The OC relay is activated when the fault current exceeds the pick-up current setting. The OC relay curve's time setting is either a definite time (DMT) or inverse time (IDMT). In

Table 1 IEC parameters of the standard relay curves of the REF 615 model [24, 28]

	α	β
Normal Inverse (IEC NI)	0.14	0.02
Very Inverse (IEC VI)	13.5	1
Extremely Inverse (IEC EI)	80	2
Short Time Inverse (IEC STI)	0.05	0.04
Long Time Inverse (IEC LTI)	120	1

the DMT curve, the fault current has a constant running time. In the IDMT relay curve, the fault current and the operating time are inversely related, i.e., the higher the fault current, the lower the operating time. The standard IDMT curves can be divided into three main inverse classes: normal inverse (NI), very inverse (VI) and extremely inverse (EI). The three classes have the same inverse relationship between the fault current and tripping time but differ in inverse degree. The VI curve is steeper than the NI curve because the tripping process quickly accelerates under the same current reduction. In OCRs with EI characteristics, the tripping time inversely related to the square of the fault current.

$$t = TDS * \frac{\alpha}{\left(\frac{I}{I_p}\right)^\beta - 1} \quad (1)$$

where t : operating time of the relay (s), TDS: time dial setting (time multiplier), I fault current (A), I_p : pick-up current (A), α, β : constants.

2.2 IEEE/ANSI standard characteristics

According to IEEE C37.112–1996 [25], other relay curves can be used to represent the relationship between OCR operating time and its detected fault current. These characteristic curves are determined by using Eq. (2). The additional parameter δ is involved only in the IEEE standard. The ANSI/IEEE standard characteristics of the relay curve are similar to those of IEC standard characteristics (Fig. 2). Table 2 lists the evaluation results of the required values of α , β and δ to obtain the ANSI/IEEE trip time characteristics of the REF 615 relay.

$$t = TDS * \left[\frac{\alpha}{\left(\frac{I}{I_p}\right)^\beta - 1} + \delta \right] \quad (2)$$

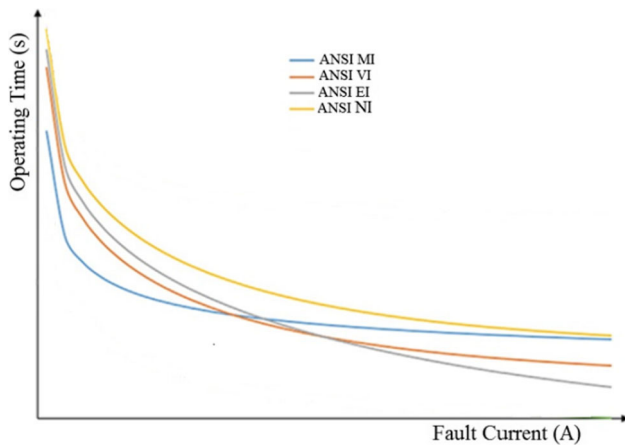


Fig. 2 IEEE characteristics of OC relay

Table 2 ANSI/IEEE parameters of the standard relay curves of the REF 615 model [25, 28]

	α	β	δ
Normal Inverse (ANSI NI)	0.0086	0.02	0.0185
Moderately Inverse (ANSI MI)	0.0515	0.02	0.114
Very Inverse (ANSI VI)	19.61	2	0.491
Extremely Inverse (ANSI EI)	28.2	2	0.1217

3 The proposed methodology

The relay cannot handle its failure when operating as the main protection with the conventional model of standard characteristics. Thus, a new method is proposed to address with this situation, and the OC relay is modified to obtain new characteristics for minimum tripping time and maximum protection level during relay failure. The proposed multi-characteristic relay in this study is based on the union of the two standard curves of normal inverse and very inverse without blocking any of their parts. The proposed technique depends on simultaneous activation of the relay settings. The method’s objective is to demonstrate the influence of using unconventional time curves to increase protection efficiency and performance by reducing operating times.

3.1 Theoretical method: mixed characteristics design in OC relay

In this study, the ANSI NI and VI curves of the REF 615 relay model are used to set up the OC relay for feeder protection against OC faults (Fig. 3). The operating area of the relay is divided into two areas. In the first area, the operating time of the NI curve is lower than that of the VI curve. In the second area, the operating time of the VI curve is lower than that of the NI curve. The proposed method has two functions as

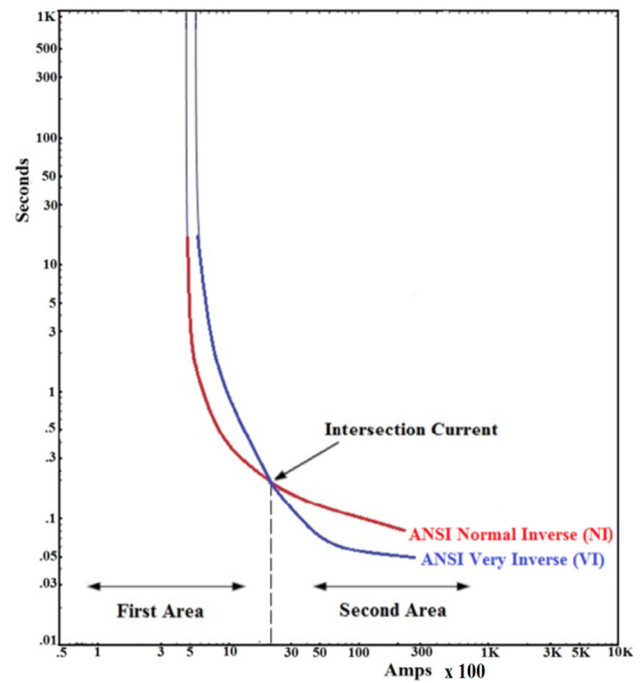


Fig. 3 The used relay curve types

shown in Fig. 3. The first function is the primary protection with minimum operating times of NI curve (red curve) in the first area and with minimum operating times of VI curve (blue curve) in the second area. In the second function, the OC relay can operate as backup protection for itself through its VI curve (blue curve) in the first area and by NI curve (red curve) in the second area. In other words, the OC relay through its VI curve can act as a backup in the first area if it is unable to detect the fault current through its NI curve and, in the second area, the OC relay through NI curve can act as a backup if it is unable to detect the fault current via its VI curve. This theory of mixing the NI and VI curves generates nonstandard curve of multi-characteristic relay capable of reducing the operating time and providing self-backup protection in the real system.

3.2 Practical method

In commercial relays, the OC relays frequently provide three distinct settings of $I>$, $I>>$ and $I>>>$ that can be set separately and individually to protect the devices. The two groups of the REF 615 model (OC1 and OC2 levels in ETAP software) are used in this study. Each group (OC level) contains two settings, namely OC and instantaneous settings, for fault currents passing through the phase. The first setting ($I>$) represents the OC setting of OC1 and is set on ANSI NI. The second setting ($I>>$) represents the OC setting of OC2 and is set on ANSI VI. The third setting ($I>>>$) is set to the instantaneous type.

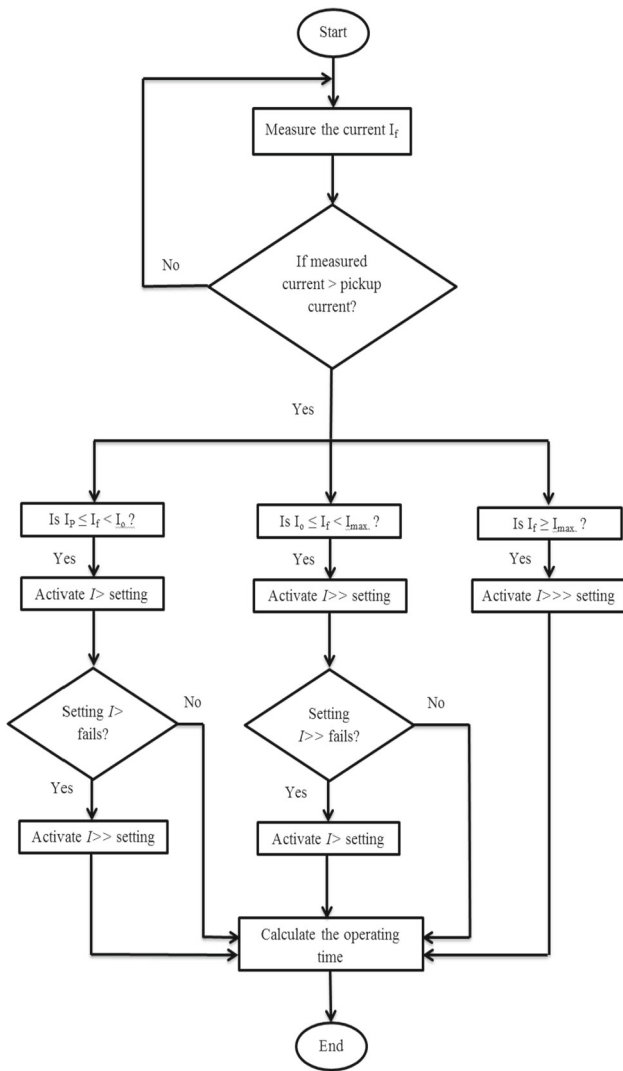


Fig. 4 Flowchart for the proposed strategy

Figure 4 shows the flowchart of the proposed strategy. The relay operates when its detected fault current exceeds its pick-up current. Under this condition, the relay activates its internal setting according to the fault current level. Each fault current level has specific time characteristics based on the standard curve used. The flowchart plan states that when the activated setting of the relay fails to operate, the proposed backup setting operates and protects the device. This implies that, in the first area, if $I>$ setting fails to operate by NI curve, the $I>>$ setting will operate as a backup through VI curve. Further, in the second area, if the $I>>$ setting fails to operate across VI curve, the $I>$ setting will operate as a backup through NI curve. Hence, the characteristic curves of NI and VI are operated and controlled by their separate settings $I>$ and $I>>$.

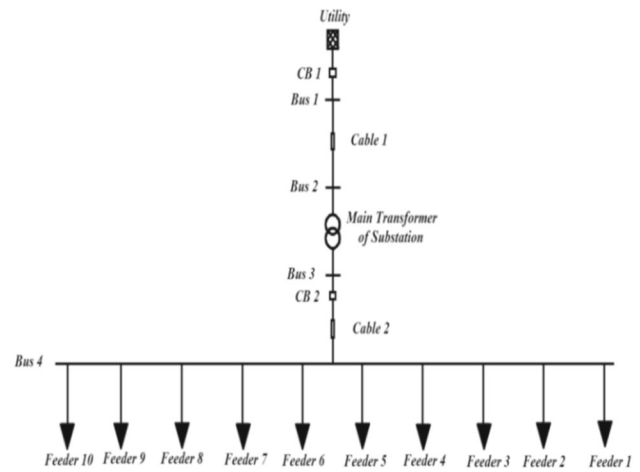


Fig. 5 Single line diagram of an actual radial system

Table 3 Consumed power by the transformer in 2020

Month	Max. Load during the month (Mw)	Min. Load during the month (Mw)
January	22	8
February	20	5
March	21	3
April	21	2
May	25	4
June	24	10
July	24	1
August	20	3
September	19	9
October	19	6
November	18	8
December	17	6

4 Tested network

In this study, the proposed technique is implemented on an actual radial system of 66/11 kV substation located at No.7, 10th of Ramadan, Egypt (Fig. 5). The actual radial system consists of a 40-MVA two-winding transformer connected to 10 feeders. Eight feeders are in service, while the others function as a backup. Each feeder is connected to certain factory and feeds its loads. Table 3 lists the actual minimum and maximum power consumed by each feeder in 2020. The percentage of the minimum and maximum loading of the transformer’s total watt power is 3% and 78%, respectively. The feeder is protected by OC relays at the factory and by the substation. The proposed time setting for the REF 615 relay model is designed to consider all variations resulting from a network configuration with light and heavy loads due to L –

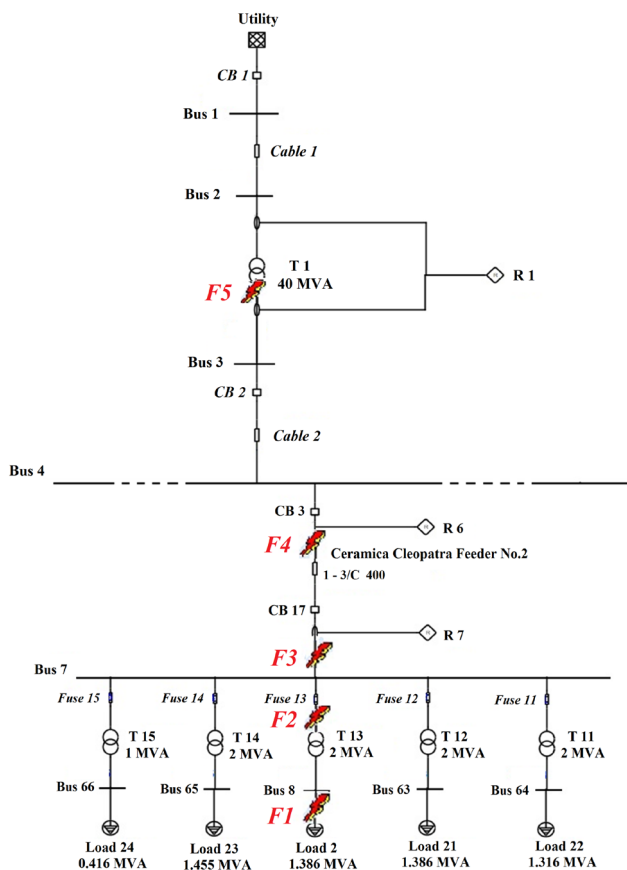


Fig. 6 Various fault locations (F1, F2, F3, F4 and F5) in the network

G, L–L, L–L–G and 3–Ph faults at various fault locations in the presence of the main transformer’s 12 Ω grounding resistance. All these variations impact the fault current level, which influences the relay’s time setting. In this research, the time-setting study is performed under these fault currents resulting from these fault conditions. Because of these fault conditions, the factory relay (FOCR) detects the range of fault currents (0.5 kA < I_f < 11 kA) when the fault location is at F1, F2 and F3 (Fig. 6). The minimum fault current for any feeder did not fall below 0.5 kA, while the maximum fault current did not rise above 11 kA. In an actual network, the conventional relay setting only uses the standard curve of ANSI NI in the coordination process. Figure 6 shows the feeder components with the possible fault locations of F1, F2, F3, F4 and F5. Feeder 7 is used as an example case study in this research to demonstrate the impact of the proposed method. The actual radial network is simulated using ETAP software (Figs. 5 and 6).

The proposed method categorizes the fault currents into three areas as shown in Fig. 7. Each area has an identified setting according to its proposed curve. The three areas are described as follows:

- i. The first area represents the range of faults currents from the minimum current (I_{min.}) to the intersection current (I_o); i.e., I_{min.} ≤ I_f < I_o. Its time is set to the NI setting (I >).
- ii. The second area denotes the range of fault currents from the intersection current (I_o) to the maximum current (I_{max.}), i.e., I_o ≤ I_f < I_{max.}. Its time is set to the VI setting (I >>).
- iii. The third area represents fault currents that are larger than the maximum current (I_{max.}), i.e., I_f ≥ I_{max.}. Its time is set to the definite time (DMT) of the instantaneous setting (I >>>).

To obtain the intersection current between the ANSI NI and VI curves (Fig. 7), the operating time of all these curves at the intersection current is equal. Therefore, the operating time equation of NI is equal to that of VI as expressed in Eq. (3).

At the intersection current, the trip time of the ANSI NI curve is equal to the trip time of the ANSI VI curve, i.e.,

$$TDS^* \left[\frac{0.0086}{\left(\frac{I}{I_p}\right)^{0.02} - 1} + 0.0185 \right] = TDS^* \left[\frac{19.61}{\left(\frac{I}{I_p}\right)^2 - 1} + 0.491 \right] \tag{3}$$

The intersection current obtained using Eq. (3) is 1.65 kA. Notably, the minimum and maximum currents are equal to the pick-up current of OC setting and the pick-up current of an instantaneous setting of the OC relay, respectively. The pick-up current (I_p) of the OC setting and that of an instantaneous setting is equal to 492 A and 7000 A, respectively. The pick-up currents of OC settings of the OC1 and OC2 levels are the same to enable the two settings (I > and I >>) to operate simultaneously during a fault. The current values of I_p, I_o and I_{max} are shown in Fig. 7. The three settings are activated in the OC relay REF 615 as shown in the proposed model in Table 4. Figure 7 shows the NI curve as the red curve, the VI curve as the blue curve and the definite time curve as the turquoise-colored curve. The operating time comprises three regions (Fig. 7) which are simulated on the logarithmic scale. The first interval represents the trip time of fault currents that are smaller than 1.65 kA. The second interval represents the trip time of fault currents in between 1.65 and 7 kA. The third interval represents the trip time of fault currents that are larger than 7 kA.

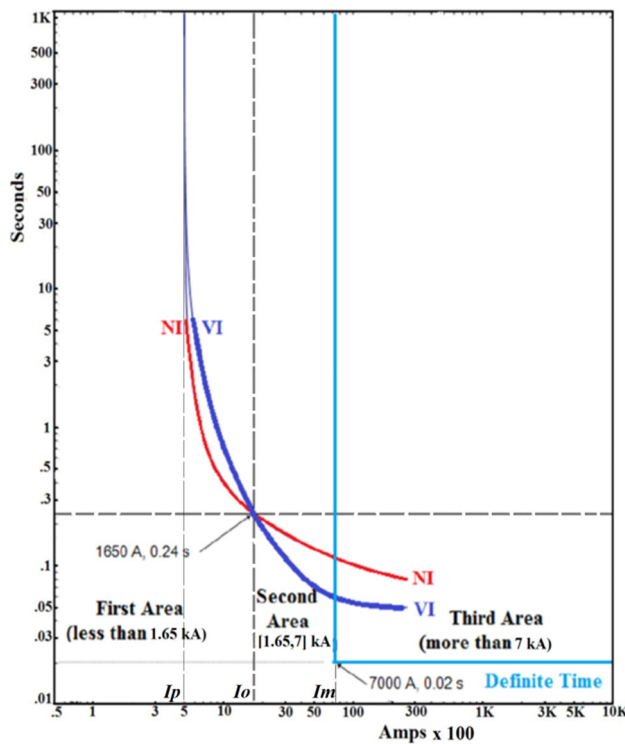


Fig. 7 Proposed three settings of the REF 615 model

Table 4 The proposed time setting

REF 615 setting	Relay curve	Setting
$I>$	NI	Pick-up current = 492 A TDS = 0.65
$I>>$	VI	Pick-up current = 492 A TDS = 0.1
$I>>>$	–	Pick-up current = 7000 A Delay time = 0.02 s

5 Results

5.1 The Effects of the proposed technique

The list in Table 5 indicates that inserting an L – G fault at $F1$ at full load results in a fault current of 0.797 kA. Here, the relay operates according to the $I>$ setting in the first area (less than 1650 A) and isolates the fault in 589 ms of operating time. In the second area, the $I>>$ setting operates at shorter operating time based on the VI curve than the NI curve. The operating times at fault currents of 5.904, 6.02, 7.193, 8.048 and 9.166 kA are reduced according to the activated settings of $I>>$ and $I>>>$, respectively. Notably, when the fault current increases, the setting degree is increased (from $I>$ to $I>>$ to $I>>>$) to reduce the operating time at

larger fault currents. The developed model demonstrates that the nonstandard relay exhibits better technical response than the standard conventional model which reduces the tripping time by about 41.07%.

In the proposed model, the relay acts as a backup for itself. To evaluate the impact of this backup, the with and without a backup setting are investigated (Table 6). The operating time is shortened in the second area when the backup setting is used. The backup setting does not work in the first area, and the primary setting (NI curve) is triggered in both systems resulting in the same tripping time.

5.2 Results of the proposed model in case of relay setting failure

In general, due to the proposed model, the main protection is automatically operated according to $I>$ setting in the first area and by $I>>$ setting in the second area. The proposed model proposes backup protection which operated by $I>>$ setting in the first area and by $I>$ setting in the second area.

Figure 8 shows the behavior of the fault currents according to the proposed model under activating the $I>$ and $I>>$ settings and failing of $I>$ setting in the two operating areas of the relay. Figure 8 shows the following:

- a) First area (less than 1.65 kA);
 - i. When the $I>$ and $I>>$ settings are activated, the relay operates by $I>$ setting via the red curve with shorter operating times. Hence, the proposed method has the ability to minimize the operating time of OC relay in the first area.
 - ii. If $I>$ setting fails to operate in the first area, the relay operates by $I>>$ setting via the green curve in longer time and protects the system. Hence, the proposed model can deal with its relay's setting failure in the first area which increases the protection level.
- b) Second area (greater than 1.65 kA);
 - i. When the $I>$ and $I>>$ settings are activated, the relay operates by $I>>$ setting via the red curve.
 - ii. If $I>$ setting fails to operate in the second area, the relay operates by $I>>$ setting via the green curve. However, the red and green curves have the same values; thus, the results remain unchanged.

Figure 9 shows the behavior of the fault currents according to the proposed model under activating the $I>$ and $I>>$ settings and failing of $I>>$ setting in the two operating areas of the relay. Figure 9 shows the following:

- a. First area (less than 1.65 kA);
 - i. When the $I>$ and $I>>$ settings are activated, the relay operates by $I>$ setting via the red curve.

Table 5 Tripping time of the relay according to the proposed technique

	Fault location	Fault type	Percentage of load	Fault current (kA)	Proposed setting	Operating time (ms)
First Area	F1	L–G	100% of full load	0.797	$I>$	589
		L–L	100% of full load	1.384	$I>$	280
Second Area		L–L–G	100% of full load	1.943	$I>>$	184
		3–Ph	80% of full load	1.964	$I>>$	181
Third Area	F3	L–L	3% of full load	5.904	$I>>$	62.9
		L–L–G	3% of full load	6.02	$I>>$	62.4
	F2	L–L	3% of full load	7.193	$I>>>$	20
		L–L–G	100% of full load	8.048	$I>>>$	20
	F3	3–Ph	100% of full load	9.166	$I>>>$	20

Table 6 Operating time with and without the proposed backup model

	Fault current (kA)	Operating time without backup (ms)	Operating time with backup (ms)
First Area	0.797	589	589
	1.384	280	280
Second Area	1.943	213	184
	1.964	211	181
	5.904	122	62.9

red and green curves have the same values; thus, the results remain unchanged.

- b. Second area (greater than 1.65 kA);
 - i. When the $I>$ and $I>>$ settings are activated, the relay operates by $I>$ setting via the red curve with shorter operating times. Hence, the proposed method has the ability to minimize the operating time of OC relay in the second area.
 - ii. If $I>>$ setting fails to operate in the second area, the relay operates by $I>$ setting via the green curve in longer time and protects the system. Hence, the proposed model can deal with its relay’s setting failure in the second area which increases the protection level.

ii. If $I>>$ setting fails to operate in the first area, the relay operates by $I>$ setting via the green curve. However, the

Fig. 8 Trip time of the proposed model when $I>$ and $I>>$ activated and when $I>$ fail

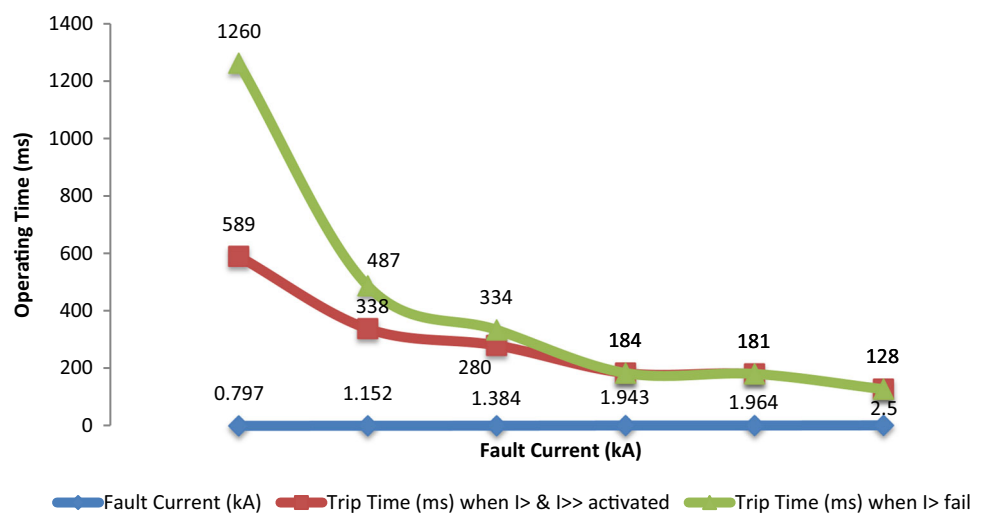
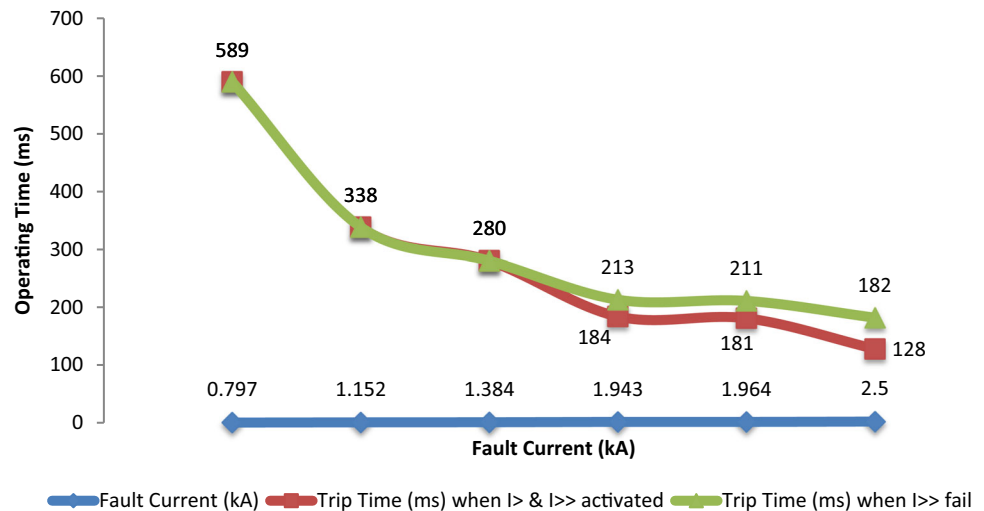


Fig. 9 Trip time of the proposed model when $I>$ and $I>>$ activated and when $I>>$ fail



5.3 Comparison study

To demonstrate the effectiveness of the developed model, the operating time of the proposed model is compared with that of the conventional model (Fig. 10) when they both operate as the primary protection. Both of the proposed and conventional models use the NI curve in the first area as a primary protection; however, the two models have different behaviors in the second area. Where, the conventional model and the proposed model use the NI and VI curves in the second area, respectively. Figure 10 shows the different behaviors of each model through red and green curves at each fault current. In the proposed model, when a fault occurs, the relay operates via the red curve with reduced tripping times due to the operation of $I>>$ setting, whereas the conventional model operates in higher tripping times via the green curve. It is demonstrated that proposed model can accurately reduce the operating time under various fault currents.

Figure 11 compares the two models when the relay fails to operate. In the proposed model, when the relay fails to operate, it operates through its proposed backup. In the first area, the $I>>$ setting operates via the red curve as a backup of $I>$ setting for fault currents lower than 1650A. In the second area, the $I>$ setting operates via the red curve as a backup of $I>>$ setting for fault currents more than 1650A. When the relay fails to operate in the conventional model, the next relay operates via the green curve, which increases the tripping time significantly. It has been demonstrated that the developed model, which has a backup mechanism, can successfully handle the relay failure, whereas the conventional model cannot. Another advantage of using the proposed technology is that it increases the likelihood that a relay will operate during a fault, and the likelihood that the location of the fault will be identified so that when the nearest relay

to the fault operates, the fault location and its cause can be quickly determined.

Figure 12 shows that the CTI of the developed model indicated by the red column and that of the conventional model indicated by the green column. The fault current in each CTI is indicated by the blue column. The results show that CTI is reduced from large time difference (green column) to a short time (red column) by about 77.98%. The results demonstrate that the presence of self-backup protection reduces the CTI between the main and backup protection. It is confirmed that the proposed model performs a rapid response, improves the relay performance, and fully protects the network in addition to providing service continuity to consumers.

6 Obtained results and major achievements

The results of this study demonstrate that in the proposed system, in addition to the other relays operating as a backup for the current relay, the relay settings also operate as a backup for themselves. According to the proposed algorithm (Fig. 3), it can be said that the tripping time behavior of OC relay has two paths: The first path of the relay is through a nonstandard curve with reduced operating times, which consists of mixed NI and VI curves as a primary protection. The second path is through the combined VI and NI nonstandard curve as a self-backup protection when any setting fails to operate. Hence, the proposed model provides the following three advantages: The first advantage is reducing the tripping times by about 41.07% (Table 5). The second advantage is the adaptive model in case of relay failure, which allows the relay to guarantee a protection backup (Figs. 8 and 9). When any relay setting fails to operate, the backup setting operates successfully and isolates the faulted line. The third

Fig. 10 The nonstandard proposed model against the standard conventional model

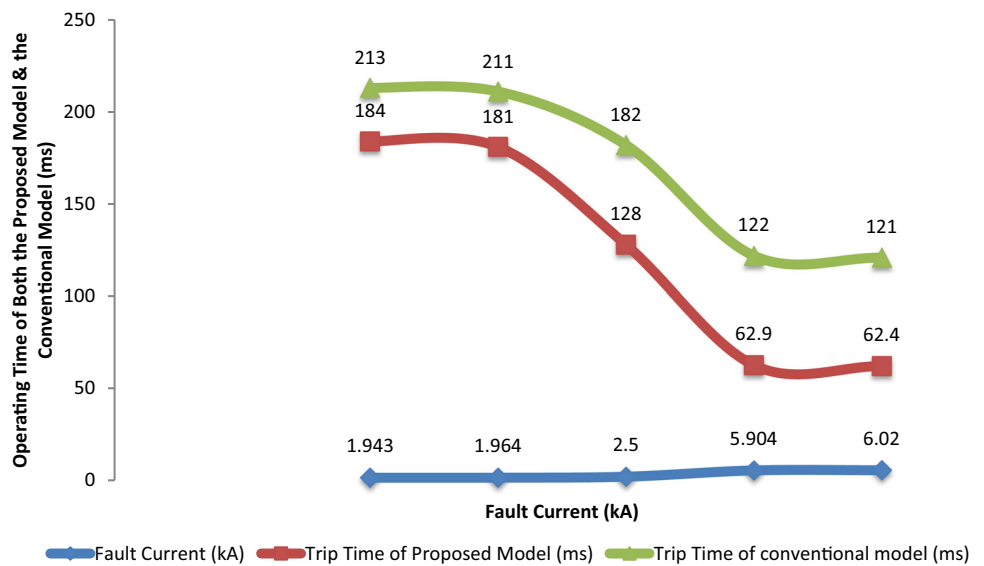
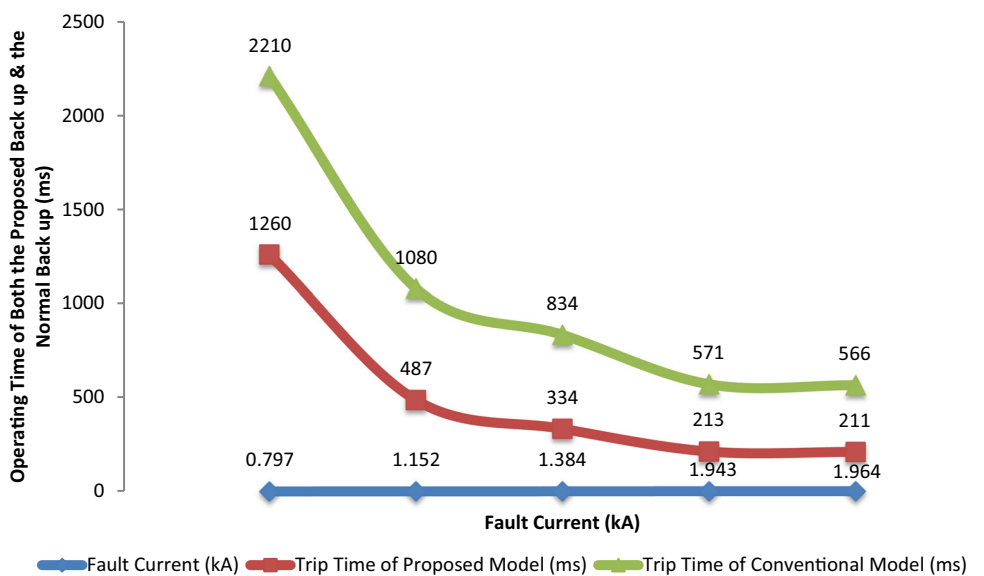


Fig. 11 Proposed model under relay failing compared with the conventional model



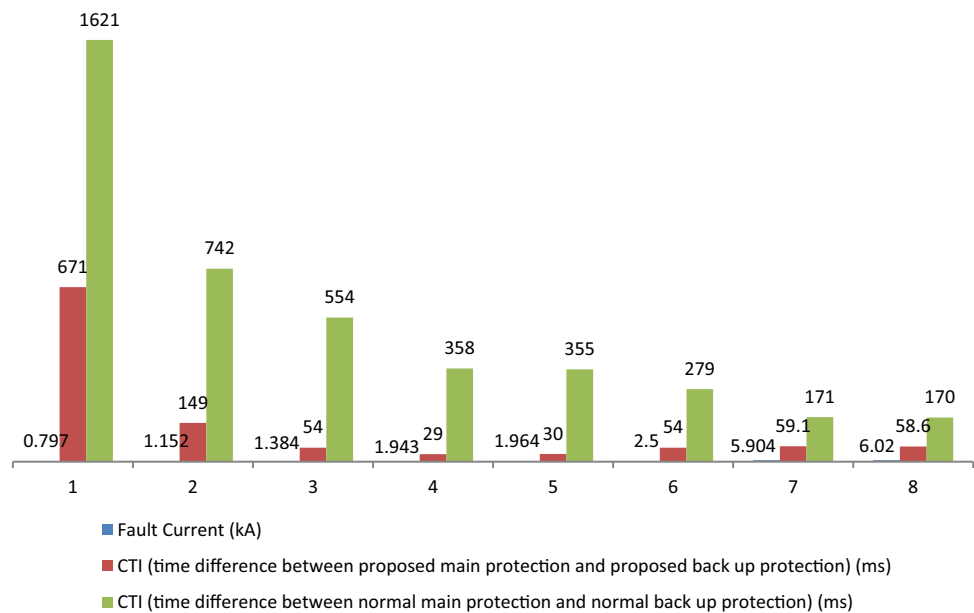
advantage is that the time difference between primary protection and backup protection (CTI) is reduced by about 77.98% (Fig. 12). Figures 10 and 11 show a comparison study between the proposed and conventional models. Previous results demonstrate that the proposed model successfully shortens the relay’s tripping time and maximizes the network’s protection level.

7 Conclusions

The proposed OC relay model is applied and tested on an actual radial system of 66/11 kV Egyptian substation located at NO.7 (S7), 10th of Ramadan, Egypt. The fault current behavior is studied using the network’s radial configuration

with light and heavy loads caused by various fault types at different locations. The results demonstrate that the modified OC relay has multi-characteristic functions. The first feature of the new characteristics is minimizing the operating time by about 41.07% compared with the standard relay. The second feature is the backup action in case of relay failure, thus increasing the protection level. In the first area, when the $I >$ setting fails, the $I >>$ setting operates as a backup. In the second area, when the $I >>$ setting fails, the $I >$ setting operates as backup for itself. In addition, this self-protection reduces the CTI by about 77.98%. The behavior of the proposed model provides rapid response, improved relay performance, maximum network protection and increased service continuity to the real system.

Fig. 12 Coordination time interval of the proposed and conventional models



Authors' contributions Manuscript is approved by all authors for publication.

Funding Open access funding provided by The Science, Technology & Innovation Funding Authority (STDF) in cooperation with The Egyptian Knowledge Bank (EKB). No funding is received from any funding agency for this research work.

Availability of data and materials Not Applicable.

Declarations

Competing interests The authors declare that they have no competing interests

Open Access This article is licensed under a Creative Commons Attribution 4.0 International License, which permits use, sharing, adaptation, distribution and reproduction in any medium or format, as long as you give appropriate credit to the original author(s) and the source, provide a link to the Creative Commons licence, and indicate if changes were made. The images or other third party material in this article are included in the article's Creative Commons licence, unless indicated otherwise in a credit line to the material. If material is not included in the article's Creative Commons licence and your intended use is not permitted by statutory regulation or exceeds the permitted use, you will need to obtain permission directly from the copyright holder. To view a copy of this licence, visit <http://creativecommons.org/licenses/by/4.0/>.

References

- Castillo-Salazar CA, Conde-Enriquez A, Schaeffer SE (2015) Directional overcurrent relay coordination considering non-standardized time curves. *Electr. Power Syst. Res.* 122:42–49
- Castillo CA, Conde A, Fernandez E (2018) Mitigation of DOCR miscoordination through distance relays and non-standard overcurrent curves. *Electr Power Syst Res* 163:242–251
- Piescorovsky EC, Schulz NN (2017) Fuse relay adaptive overcurrent protection scheme for microgrid with distributed generators. In: *IET generation, transmission & distribution, institution of engineering and technology*, pp 540–549
- Boucekara HREH, Zelligui M, Abido MA (2017) Optimal coordination of directional overcurrent relays using a modified electromagnetic field optimization algorithm. *Appl Soft Comput* 54:267–283
- Noghabi AS, Mashhadi HR, Sadeh J (2010) Optimal coordination of directional overcurrent relays considering different network topologies using interval linear programming. *IEEE Trans Power Deliv* 25:1348–1354
- Costa MH, Ravetti MG, Saldanha RR, Carrano EG (2019) Minimizing undesirable load shedding through robust coordination of directional overcurrent relays. *Int J Electr Power Energy Syst* 113:748–757
- Momesso AEC, Bernardes WMS, Asada EN (2019) Fuzzy adaptive setting for time-current-voltage based overcurrent relays in distribution systems. *Int J Electr Power Energy Syst* 108:135–144
- Chabanloo RM, Abyaneh HA, Agheli A, Rastegar H (2011) Overcurrent relays coordination considering transient behaviour of fault current limiter and distributed generation in distribution power network. In: *IET generation, transmission & distribution, institution of engineering and technology*, pp 903–911
- Mehrjerdi H, Ghorbani A (2017) Adaptive algorithm for transmission line protection in the presence of UPFC. *Int J Electr Power Energy Syst* 91:10–19
- Kumar DS, Srinivasan D, Sharma A, Reindl T (2018) Adaptive directional overcurrent relaying scheme for meshed distribution networks. *IET GTD* 12(13):3212–3220
- Shih MY, Conde A, Leonowicz Z, Martirano L (2017) An adaptive overcurrent coordination scheme to improve relay sensitivity and overcome drawbacks due to distributed generation in smart grids. *IEEE Trans Ind Appl* 53(6):5217–5228
- Ojaghi M, Mohammadi V (2018) Use of clustering to reduce the number of different setting groups for adaptive coordination of overcurrent relays. *IEEE Trans Power Deliv* 33(3):1204–1212
- Samadi A, Chabanloo RM (2020) Adaptive coordination of overcurrent relays in active distribution networks based on independent

- change of relays' setting groups. *Int J Elec Power Energy Syst* 120:106026
14. Darabi A, Bagheri M, Gharehpetian GB (2020) Highly reliable overcurrent protection scheme for highly meshed power systems. *Int J Elec Power Energy Syst* 119:105874
 15. Saleh KA, Zeineldin H, Al-Hinai A, El-Saadany EF (2014) Optimal coordination of directional overcurrent relays using a new time–current–voltage characteristic. *IEEE Trans Power Deliv* 30(2):537–544
 16. Chaitusaney S, Yokoyama A (2008) Prevention of reliability degradation from recloser–fuse miscoordination due to distributed generation. *IEEE Trans Power Deliv* 23(4):2545–2554
 17. Nascimento JP, Brito NS, Souza BA (2020) An adaptive overcurrent protection system applied to distribution systems. *Comput Electr Eng* 81:106545
 18. Singh M, Vishnuvardhan T, Srivani SG (2016) Adaptive protection coordination scheme for power networks under penetration of distributed energy resources. *IET Gener Transm Distrib* 10(15):3919–3929
 19. Papaspiliotopoulos VA, Korres GN, Hatziargyriou ND. Protection coordination in modern distribution grids integrating optimization techniques with adaptive relay setting. In: 2015 IEEE Eindhoven PowerTech; 2015. pp. 1–6.
 20. Shih MY, Salazar CAC, Enríquez AC (2015) Adaptive directional overcurrent relay coordination using ant colony optimisation. *IET Gener Transm Distrib* 9(14):2040–2049
 21. Saleh KA, Moursi MSE, Zeineldin HH (2015) A new protection scheme considering fault ride through requirements for transmission level interconnected wind parks. *IEEE Trans Ind Inf* 11(6):1324–1333
 22. Ojaghi M, Sudi Z, Faiz J (2013) Implementation of full adaptive technique to optimal coordination of overcurrent relays. *IEEE Trans Power Deliv* 28(1):235–244
 23. Rahmati A, Dimassi MA, Adhami R, Bumblauskas D (2015) An overcurrent protection relay based on local measurements. *IEEE Trans Ind Appl* 51(3):2081–2085
 24. I. Std, 60255–3, Electrical relays-Part 3: Single input energizing quantity measuring relays with dependent or independent time (1989).
 25. I. Std, C37. 112–1996, IEEE standard inverse-time characteristic equations for overcurrent relays (1997)
 26. Kiliçkiran HC, Sengör I, Akdemir H, Kekezoğlu B, Erdinc O, Paterakis NG (2018) Power system protection with digital overcurrent relays: a review of non-standard characteristics. *Electric Power Syst Res* 164:89–102
 27. ALSTOM, Network protection & automation guide, Alstom (2002)
 28. SIEMENS, Siprotec 5 overcurrent protection 7sj82/7sj85. <https://new.siemens.com/global/en/products/energy/energy-automation-and-smart-grid/protection-relays-and-control/siprotec-5.html> 2020.

Publisher's Note Springer Nature remains neutral with regard to jurisdictional claims in published maps and institutional affiliations.